Stat Papers (2013) 54:1095–1107
DOI 10.1007/s00362-013-0538-6

REGULAR ARTICLE

EEG in the diagnostics of Alzheimer's disease

M. Waser · M. Deistler · H. Garn · T. Benke · P. Dal-Bianco · G. Ransmayr · D. Grossegger · R. Schmidt

Received: 23 April 2013 / Revised: 30 May 2013 / Published online: 14 June 2013

Abstract Dementia caused by Alzheimer's disease (AD) is worldwide one of the main medical and social challenges for the next years and decades. An automated analysis of changes in the electroencephalogram (EEG) of patients with AD may contribute to improving the quality of medical diagnoses. In this paper, measures based on uni- and multi-variate spectral densities are studied in order to measure slowing and,

M. Waser (✉) · H. Garn
AIT Austrian Institute of Technology, Donau-City-Strasse 1, 1220 Vienna, Austria
e-mail: markus.waser@ait.ac.at

H. Garn
e-mail: heinrich.garn@ait.ac.at

M. Deistler
Department of Mathematical Methods in Economics, Vienna University of Technology,
Argentinierstrasse 8/2 E105-2,
1040 Vienna, Austria
e-mail: manfred.deistler@tuwien.ac.at

T. Benke
Department of Neurology, Medical University of Innsbruck,
Innrain 52, 6020 Innsbruck, Austria
e-mail: thomas.benke@uki.at

P. Dal-Bianco
Department of Neurology, Medical University of Vienna,
Währinger Gürtel 18-20, 1090 Wien, Austria
e-mail: peter.dal-bianco@meduniwien.ac.at

G. Ransmayr
Department of Neurology, General Hospital Linz,
Krankenhausstrasse 9, 4021 Linz, Austria
e-mail: gerhard.ransmayr@akh.linz.at

in greater detail, reduced synchrony in the EEG signals. Hereby, an EEG segment is interpreted as sample of a (weakly) stationary stochastic process. The spectral density was computed using an indirect estimator. Slowing was considered by calculating the spectral power in predefined frequency bands. As measures for synchrony between single EEG signals, we analyzed coherences, partial coherences, bivariate and conditional Granger causality; for measuring synchrony between groups of EEG signals, we considered coherences, partial coherences, bivariate and conditional Granger causality between the respective first principal components of each group, and dynamic canonic correlations. As measure for local synchrony within a group, the amount of variance explained by the respective first principal component of static and dynamic principal component analysis was investigated. These measures were exemplarily computed for resting state EEG recordings from 83 subjects diagnosed with probable AD. Here, the severity of AD is quantified by the Mini Mental State Examination score.

Keywords Alzheimer's Disease · Electroencephalogram · Spectral density estimation · Coherence · Partial coherence · Granger causality · Canonical correlation

1 Introduction

1.1 Alzheimer's disease

Dementia is worldwide one of the main medical and social challenges for the next years and decades. In Austria at present about 120,000 people are suffering from dementia and the forecast is that in the year 2050 approximately 262,300 persons will be affected (Schmidt et al. 2010). The main cause for demential syndromes is Alzheimer's disease (AD) which is responsible for approximately 60 % of dementia cases (Knopman et al. 2003).

To this day, there is no cure for AD, and its cause and progression are not well understood. Research indicates that the cause of AD is associated with plaques and tangles in the brain (Moreira et al. 2009). "Mild cognitive impairmen" (MCI) can be an early symptom for later dementia. Some MCI patients decline very slow, but others progress to dementia within a few years. In progressive cases, early detection is desirable. Today, diagnostic procedures consist mainly of neuropsychological testing, such as the Mini Mental State Examination (MMSE) (Folstein et al. 1975) used in this paper. In certain cases magnetic resonance imaging (MRI) is used for detectingatrophy of the hippocampi, the medial temporal lobes and the total brain volume

D. Grossegger
B.E.S.T. Medical Systems, Dr. Grossegger & Drbal GmbH,
Ruthgasse 19/1, 1190 Wien, Austria
e-mail: office@alphatrace.at

R. Schmidt
Department of Neurology, Medical University of Graz,
Auenbruggerplatz 22, 8036 Graz, Austria
e-mail: reinhold.schmidt@medunigraz.at

(Thompson and Toga 2009). Reduced glucose metabolism in specific regions of the brain as visualized by fluordesoxyglucose positron emission tomography (FDG PET) is another indicator for AD (Pupi et al. 2009). Several clinical studies suggest that carriers of the apolipoprotein E (APOE $\epsilon 4$) have an increased risk for contracting the disease (Moreira et al. 2009).

Additionally, research is conducted on functional magnetic resonance imaging (fMRI) (Sakoglu 2011; Liu 2008), and finally on the electroencephalogram (EEG) (Jeong 2004; Dauwels et al. 2010), the latter being the focus of this paper.

1.2 EEG in AD diagnosis

When using EEG in clinical practice today, most common is visual analysis performed by medical experts. Commercial software tools are typically used to perform semi-automatic analyses of absolute and relative power spectra, mean frequency and coherence. More advanced, computer-aided procedures may significantly contribute to improving the quality of diagnosing. In diagnosis of AD, the major benefits of EEG over MRI or PET are its non-invasiveness, easy application and low cost.

Clinical studies have examined the following EEG characteristics of patients with AD and found them to be helpful in supporting medical diagnosis (Jeong 2004):

- Slowing
- Reduced complexity
- Reduced synchrony

In this paper, the focus is on methods based on spectral densities with a special focus on the multivariate case. We consider slowing and, in greater detail, reduced synchrony. The purpose is not to provide a detailed description of the results of a clinical study, but to give an overview of the methods and a number of examples instead.

1.3 Structure of this paper

Section 2 is concerned with a short description of the EEG data used for our analyses. In Sect. 3 we discuss artefacts and their removal from the EEG. Section 4 is concerned with slowing of EEG, that can be particularly seen in the estimated spectral density. Section 5 focuses on quantifying synchrony by measures such as coherence, partial coherence, dynamic canonical correlation analysis, Granger causality and conditional Granger causality. All these measures are based on the multivariate spectral density corresponding to all EEG channel signals, the major question being thereby the relation of these measures to the severity of AD as quantified by MMSE. Section 6 provides a short conclusion.

2 Description of the data

For the present study, EEG recordings from the PRODEM-AUSTRIA[1] database of the Austrian Alzheimer Society were used. More specifically, the EEG samples were

[1] http://www.alzheimer.mcw-portal.com/index.php?id=27.

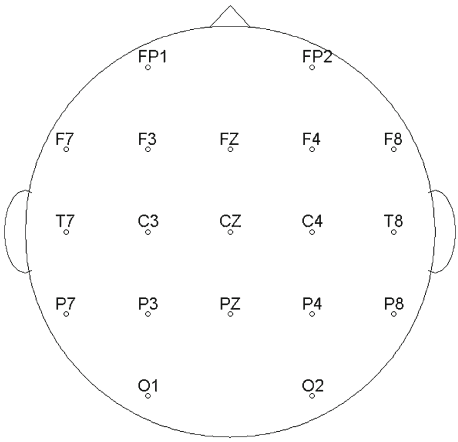

Fig. 1 Electrode names and positions

recorded at the Medical Universities of Graz, Innsbruck, Vienna and the General Hospital Linz, all complying with a homogeneous study protocol. The sample consists of EEG recordings from 83 subjects (48 female, 35 male) diagnosed with probable AD as defined by the NINCDS-ADRDA criteria (McKhann et al. 1984). All subjects underwent neuropsychological assessments including MMSE (Folstein et al. 1975) and other neuropsychological assessments. Throughout this work, the MMSE score - clinically well-established for evaluating cognitive impairment - is used to quantify the progress of AD. MMSE scores range on an ordinal scale from 30 to 0 where lower scores indicate more severe cognitive impairment. Only study subjects reaching MMSE scores between 26 and 15 were considered, the average score was 22.06 ($\pm$3.18). Age, sex, duration of AD, and degree of education are applied as confounding variables for further statistical analyses.

The EEG data were recorded and digitalized using the NeuroSpeed software of the alpha-trace digitalEEG System[2] with sampling rate 256 Hz and analog bandpass filtering in the range 0.3–70 Hz. Nineteen electrodes were positioned on the subjects' scalp according to the international 10–20 system (Jasper 1958). The channel names and positions are illustrated in Fig. 1. Channels starting with an "F" are on frontal positions, channels starting with a "T" are on temporal positions, those starting with a "P" are on parietal, and channels starting with an "O" are on occipital positions. Connected mastoids were used as reference and the ground electrode was located between channels Fz and Cz. Additionally, both horizontal and vertical electroocculogram (EOG) channels and an electrocardiogram (ECG) channel were recorded. Impedances were kept below 10 kΩ.

The EEG segments used for this work were recorded with the subjects sitting in a resting but awake condition with eyes closed for 3 min.

3 Artefacts in EEG

The main artefacts occuring in EEG data are the following:

[2] http://www.alphatrace.at.

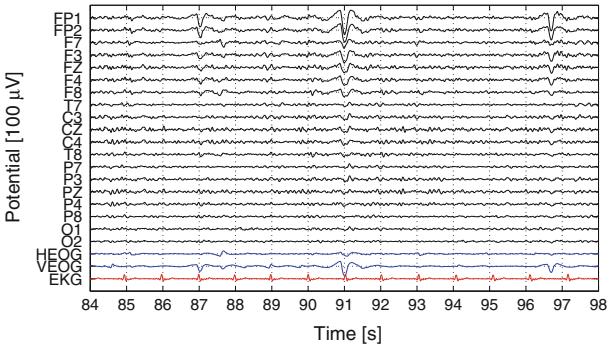

Fig. 2 Blink-artefacts in frontal EEG channels

- Eye-artefacts including blinking and eye movements
- Artefacts from the heart beat
- Artefacts from other muscles/movement
- Technical artefacts, e.g. from bad electrode contacts

Because the EOG data are available and have practically no dynamic influence on the EEG data, the eye-artefacts can be removed by static linear regression on the EOG data. In order to eliminate high-frequency signal components in the EOG channels that are not associated with eye movements but origin from brain signals, the EOG signals are subject to prior lowpass filtering. Figure 2 shows an EEG segment with eye-artefacts in several channels. The upper channels correspond to frontal electrode positions, here the EEG signals are corrupted the most by the artefacts.

Artefacts from heart-beat are more difficult to remove. The heartbeat rates of the ECG are in the range of 1–2.5 Hz. However, because of its spiked form, there are significant superharmonics influencing the EEG signals of interest. A method for properly removing these artefacts is described in Waser and Garn (2013). Figure 3 shows an EEG segment with artefacts from heart-beat in all EEG channels and also in the horizontal EOG channel. In Fig. 3, the signal at the bottom is the ECG that

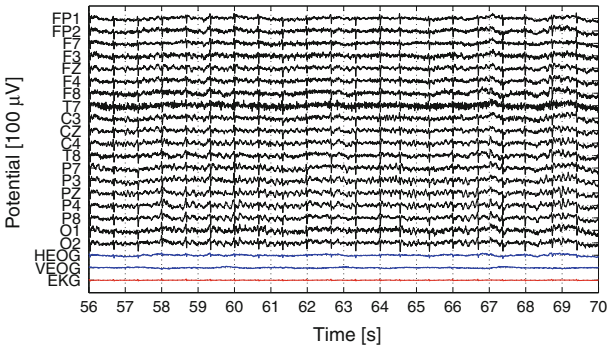

Fig. 3 Heart beat artefacts in all EEG channels

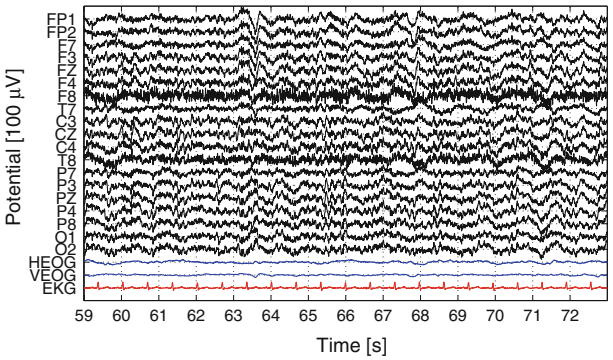

Fig. 4 Artefacts from muscle tension in EEG channels F8 and T8

measures the potential induced by the heart beat (in different scale than the EEG channels).

Artefacts from other muscles are typically corrupting the frequency range above 15 Hz. In Fig. 4, two channels (F8 and T8) are corrupted by high-frequency artefacts caused by muscle tension. Therefore, the EEG signals are subject to lowpass filtering at 15 Hz.

The artefact-corrected EEG signals are divided in intervals of 4 s with 2 s overlap. Those EEG segments that contain other artefacts that cannot be removed (e.g. artefacts from bad electrode contacts) are excluded from further analyses.

4 Slowing

4.1 General remarks

A feature that could be helpful in supporting medical diagnosis of AD is a slow-down in frequency of the EEG signal. To be more precise, a segment of the EEG is here interpreted as a sample of a (weakly) stationary stochastic process $(x_t)_{t\in\mathbb{Z}}$. Under the assumption that the second moments $\gamma_s = \mathbb{E}x_{t+s}x_t$ are absolutely summable, the spectral density $f(\lambda) = (2\pi)^{-1}\sum \gamma_s\, e^{-i\lambda s}$ exists and is in one-to-one relation with the second moments of the process. In particular, $\gamma_0 = \int f(\lambda)\, d\lambda$ and thus $\int_a^b f(\lambda)\, d\lambda$ is a measure of the contribution of the frequency band $[a, b]$ to the overall variance γ_0 of the process. For more details on spectral estimation see Brillinger (1981). Significant changes observable in the course of the disease are an increase in delta (2–4 Hz) and theta activity (4–8 Hz) and a decrease in alpha (8–12 Hz) and beta activity (12–30 Hz) (Jeong 2004).

Three common procedures for estimating the spectral density are the following: the periodogram, (consistent) indirect spectral estimation, and AR-fitting using Yule–Walker equations and the AIC criterion (Akaike 1974). In this context the interest is in estimating the power in the respective frequency bands rather than in estimating the spectral density itself. Note that the cumulative periodogram is a consistent estimator of the spectral distribution function and thus it is suited for estimating the power in

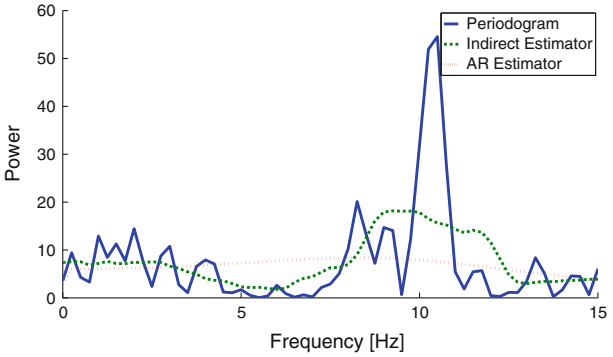

Fig. 5 Spectral density estimation: periodogram, indirect estimator, AR-based estimator

frequency bands. An indirect spectral estimator improves the quality of estimating the spectral density, but the difference in estimating the spectral distribution is neglectable in our case. In our case, the AR-based procedure is less suited for estimation, as it approximates global rather than local characteristics of the true underlying spectrum and thus the frequency bands of interest between 2–30 Hz are influenced by non-relevant frequency bands above 30 Hz. (Note that the Nyquist frequency is 128 Hz.) Figure 5 shows an example for the spectral estimators on a 4 s EEG segment. Although the periodogram-based and the indirect estimation differ on the single frequencies, the relative powers in the aforementioned frequency bands are similar.

In resting state with closed eyes, a dominant alpha peak typically occurs in the spectrum of the parietal and occipital EEG channels. This peak is caused by the so-called alpha waves, neural oscillations in the frequency range of 8–12 Hz arising from synchronous electrical activity of thalamic neurons. For patients suffering from AD, a shift of this peak to lower frequencies within the alpha frequency band might be another indicator for slowing. The spectral alpha peak is illustrated by the example in Fig. 6. It shows the spectral density of a parietal channel segment in two different states, resting state with eyes closed and with eyes opened. In the latter case the alpha waves are suppressed and therefore there is no dominant spectral alpha peak visible. Both spectra were estimated using an indirect spectral estimator.

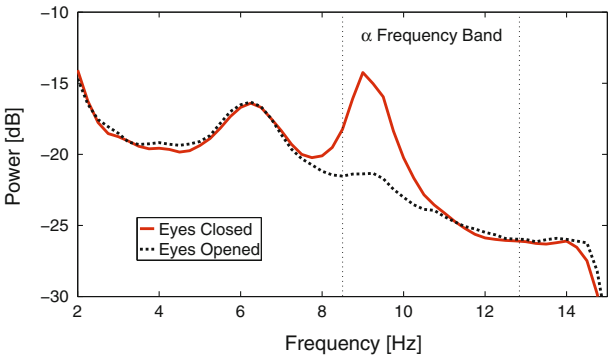

Fig. 6 Power spectral density: eyes closed versus eyes opened

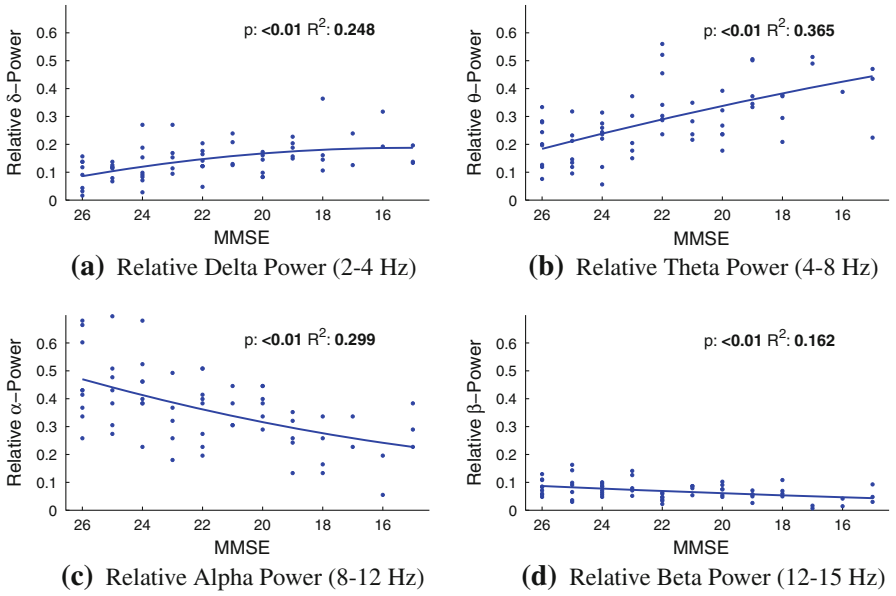

Fig. 7 Example for slowing: relative power in different frequency bands

4.2 Examples

As an example of slowing, Fig. 7 shows the powers in the aforementioned frequency bands relative to the overall power versus MMSE scores by scatterdiagrams. A quadratic regression has been fitted to these scatterdiagrams. The relative powers in the low frequency ranges delta (Fig. 7a) and theta (Fig. 7b) increase, while those in the higher frequency ranges alpha (Fig. 7c) and beta (Fig. 7d) decrease. In this example, the co-variables age, sex, degree of education, and duration of dementia were taken into account where age and duration of dementia are introduced via both linear and quadratic terms. In order to evaluate the significancy and goodness of fit, we used the p- and R^2-values.

5 Reduced synchrony

5.1 General remarks

In this section, the focus is on investigating the influence of AD on the degree of functional connectivity between cortical areas. Functional connectivity is investigated between channels as well as between groups of channels. In the latter case, the following groups were defined Dauwels et al. (2010): Anterior (FP1, FP2, F3, F4), Central (FZ, C3, CZ, C4, PZ), Posterior (P3, P4, O1, O2), Temporal Left (F7, T7, P7), and Temporal Right (F8, T8, P8). As far as single channels are concerned, we analysed (bivariate) coherence, partial coherence, bivariate and conditional Granger causality. For each region, a (static) PCA has been performed. For the respective first

principal components, coherences, partial coherences, Granger causality, and conditional Granger causality have been investigated. In addition, dynamic canonical correlation analysis has been performed. Finally, as a measure for the degree of local synchrony, the amount of variance explained by the first principal component of a dynamic PCA relative to the total variance has been considered for each group of channels. All these measures derived from the multivariate spectral density are not considered for single frequencies, but are averaged over the aforementioned frequency bands.

5.2 Measures for synchrony

Consider an n-dimensional multivariate stationary process $(x_t)_{t\in\mathbb{Z}}$ with covariances $\gamma_s = \mathbb{E}x_{t+s}x_t'$ and spectral density matrix $f(\lambda) = (2\pi)^{-1}\sum \gamma_s\, e^{-i\lambda s}$ with $f = (f_{ij}),\ i, j = 1\ldots n$. The spectral density was estimated with an indirect procedure using a Parzen window in order to guarantee that the estimate is positive semi-definite.

Coherences are used as measures for mutual (linear, dynamic) dependence between univariate subprocesses corresponding to the channels in our case. The squared coherence between the ith and the jth subprocess at frequency λ is defined as (see Brillinger 1981)

$$C_{ij}^2(\lambda) = \frac{|f_{ij}(\lambda)|^2}{f_{ii}(\lambda)f_{jj}(\lambda)} \tag{1}$$

$C_{ij}^2(\lambda)$ is normalized to be between 0 and 1 and is a measure of the strength of the linear coupling between channel i and j at frequency λ. Our estimator of $C_{ij}^2(\lambda)$ is based on the spectral estimate mentioned above.

In the coherence measure described above, indirect couplings between channel i and j (i.e. couplings via other channels) are taken into account as well. In order to measure the direct couplings only, i.e. couplings after removing the influence of the channels other than i or j, the so-called partial coherence (see Brillinger 1981; Flamm et al. 2012; Dahlhaus et al. 1997) was estimated. Let $g = (g_{ij}) = f^{-1}$ denote the inverse of the spectral density of the underlying stationary process (here f is assumed to be non-singular for all frequencies λ), then the squared partial coherences are defined as

$$R_{ij}^2(\lambda) = \frac{|g_{ij}(\lambda)|^2}{g_{ii}(\lambda)g_{jj}(\lambda)} \tag{2}$$

Whereas coherences and partial coherences are symmetric measures, we also considered Granger causality for measuring directed couplings. Both Granger causalities and conditional Granger causalities, i.e. with the influence of other channels removed, are suited in this context (see Flamm et al. 2012). Granger causality between two channels can be derived from a bivariate autoregressive model for these channels: The jth component is not Granger causal for the ith component, if all coefficients corresponding to the lagged jth component in the equation for the ith component are equal to zero. Conditional Granger causality is defined from an autoregressive model of order p for the n (i.e. 19 in our case) dimensional process (x_t):

$$x_t = a_1 x_{t-1} + \cdots + a_p x_{t-p} + \epsilon_t \tag{3}$$

where the stability condition is satisfied. The jth component is not conditionally Granger causal for the ith component, if all (i, j)-entries, $a_k(i, j), k = 1, \ldots, p$ of the a_k equal zero. As a measure of the degree of conditional Granger causality, we used the Euclidean norm $\sqrt{\sum_{k=1}^{p} a_k^2(i, j)}$. The analogous measure was used for "ordinary" Granger causality.

In order to describe synchrony between groups of channels, a (static) principal component analysis (PCA) was performed for each group. In this way, couplings between the groups can be approximately described via the couplings between the respective first principal components. In particular, coherences, partial coherences, Granger causality, and conditional Granger causality were considered. Additionally, static and dynamic canonical correlation analysis was used as measure of synchrony between groups of channels. The dynamical correlations between two groups of channels are defined as follows (Brillinger 1981): Let f_1 be the spectral density matrix corresponding to the channels of group 1, and f_2 the spectral density matrix corresponding to the channels of group 2. Further, let f_{21} denote the cross-spectral density between group 2 and 1. Then the dynamical correlations are defined as the (complex) singular values of $f_2^{-\frac{1}{2}} f_{21} f_1^{-\frac{1}{2}}$.

In order to measure couplings within each group of channels, static and dynamic PCA has been performed for the channels of the respective group. Dynamic PCA (see Brillinger 1981) is based on an eigenvalue decomposition of the spectral density corresponding to a group of channels. The amount of variance explained by the first principal component is a measure of the homogeneity of the group.

5.3 Examples

As example of decreasing synchrony between single channels, Fig. 8 shows the squared coherence between the channels C4 and O2 averaged in the alpha frequency band over the MMSE scores by a scatterdiagram. The same co-variables as before, namely age,

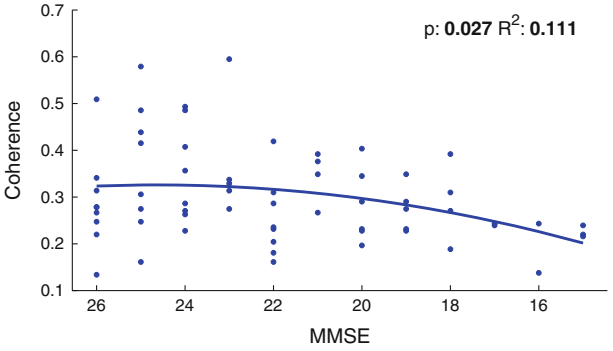

Fig. 8 Example for synchrony: *squared* coherence between C4 and O2 in alpha-band (8–12 Hz)

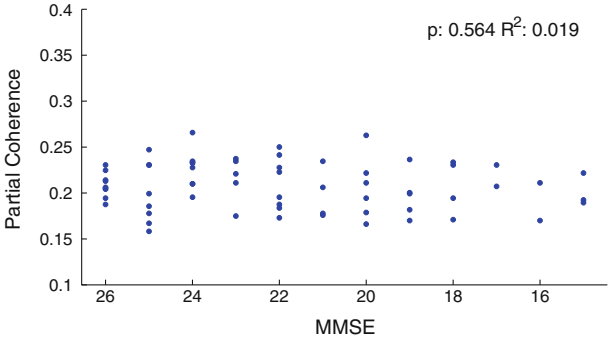

Fig. 9 Example for synchrony: partial coherence between C4 and O2 in alpha-band (8–12 Hz)

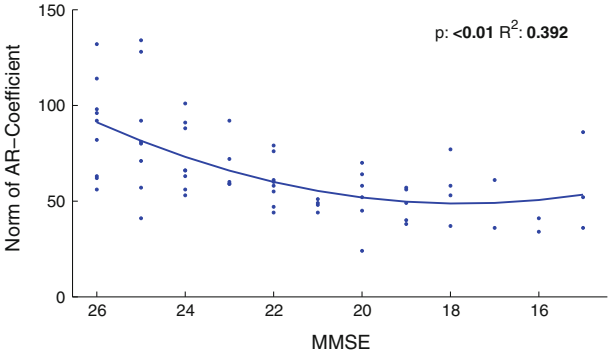

Fig. 10 Example for synchrony: Granger causality between the first factors of central and posterior region

sex, degree of education, and duration of dementia, were taken into account. For the quadratic least-squares regression the p- and R^2-values are given. In this example, we observe a slight decrease of coherence with decreasing MMSE.

In order to provide an example for the direct coupling between the same channels—C4 and O2—as before, Fig. 9 shows the partial coherence averaged in the alpha frequency band over the MMSE as scatterdiagram. Here, no significant quadratic trend ($p = 0.564 > 0.05$) can be observed.

Instead of measuring couplings between single electrodes, Fig. 10 shows the conditional Granger causality between the central electrodes and the posterior electrodes versus MMSE and with quadratic regression using the same co-variables as before. In this example, a significant decrease of Granger causality with decreasing MMSE can be observed; the R^2-value of the quadratic regression equals 0.392. Thus, as preliminary result, conditional Granger causality between different groups of channels gives promising results for decline of synchrony with decreasing MMSE.

Finally, as example for changes in synchrony within a group of channels, Fig. 11 shows the amount of variance explained by the first principal component of dynamic PCA in the posterior region. We observe a slight increase of the variance contribution of the first factor for MMSE values ranging from 26 to 22, followed by a slight decrease for MMSE values below 22.

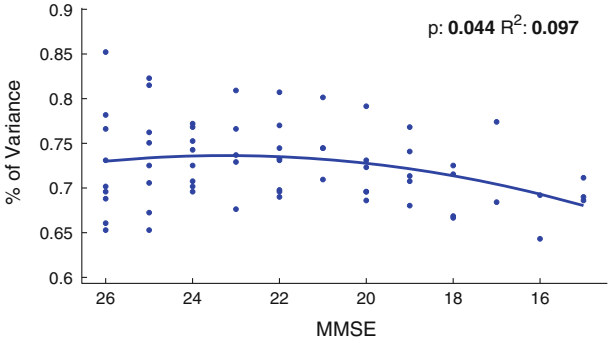

Fig. 11 Example for synchrony: information described by the first factor of a dynamic PCA in the posterior region

6 Conclusion

In this paper, we described measures based on spectral densities of uni- and multivariate EEG signals that may contribute to improving the quality of diagnosing AD. In particular, slowing in univariate spectral densities, and, for the multivariate case, spectral based measures for synchrony, namely coherences, partial coherences, Granger causalities, conditional Granger causalities, dynamic canonic correlations, and static and dynamic PCA were investigated.

Acknowledgments Part of this work has been supported by the project *A*dvanced EEG in der Vorhersage des Verlaufs der Alzheimerdemenz, Austrian Research Promotion Agency (FFG), Project ID 827462. The EEG data has been provided by the Medical University of Graz, the Medical University of Innsbruck, the Medical University of Vienna, and the General Hospital Linz.

References

Akaike H (1974) A new look at the statistical model identification. IEEE Trans Autom Control 6(19):716–723

Brillinger DR (1981) Time series: data analysis and theory. Holden-Day, San Francisco

Dahlhaus R, Eichler M, Sandkühler J (1997) Identification of synaptic connections in neural ensembles by graphical models. J Neurosci Methods 77:93–107

Dauwels J, Vialatte F, Cichocki A (2010) Diagnosis of Alzheimer's disease from EEG Signals: where are we standing? Curr Alzheimer Res 6(7):487–505

Flamm C, Kalliauer U, Deistler M, Waser M (2012) System identification, environmental modelling, and control system design, graphs for dependence and causality in multivariate time series. Springer, London, pp 133–151

Folstein MF, Folstein SE, McHugh PR (1975) 'Mini-mental state'. A practical method for grading the cognitive state of patients for the clinician. J Psychiatric Res 3(12):189–198

Jasper HH (1958) The ten-twenty electrode system of the International Federation. Electroencephalogr Clin Neurophysiol 2(10):371–375

Jeong J (2004) EEG dynamics in patients with Alzheimer's disease. Clin Neurophysiol 4(115):1490–1505

Knopman DS, Boeve BF, Petersen RC (2003) Essentials of the proper diagnoses of mild cognitive impairment, dementia, and major subtypes of dementia. Mayo Clin Proc 10(78):1290–1308

Liu Y et al (2008) Regional homogeneity, functional connectivity and imaging markers of Alzheimer's disease: a review of resting-state fMRI studies. Neuropsychologica 46:1648–1656

McKhann G, Drachman D, Folstein M, Katzman R, Price D (1984) Stadlan E. Clinical diagnosis of Alzheimer's disease: report of the NINCDS-ADRDA work group under the auspices of Department of Health and Human Services Task Force on Alzheimer's Disease. Neurology 7(34):939–944

Moreira PI, Zhu X, Smith MA, Perry G (2009) Alzheimer's disease: an overview. Encyclopedia of neuroscience. Academic Press, In, pp 259–263

Pupi A, De Cristofaro M, Nacmias B, Sorbi S, Mosconi L (2009) Brain glucose metabolism: age, Alzheimer's disease and APoE allele effects. Encyclopedia of neuroscience. Academic Press, In, pp 363–373

Schmidt R, Marksteiner J, Dal Bianco P, Ransmayr G, Bancher C, Benke T, Wancata J, Fischer P, Leblhuber CF (2010) Konsensusstatement "Demenz 2010"der Österreichischen Alzheimer Gesellschaft. Neuropsychiatrie 24(2):67–87

Sakoglu Ü et al (2011) Paradigm shift in translational neuroimaging of CNS disorders. Biochem Pharmacol 81:1374–1387

Thompson PM, Toga AW (2009) Alzheimer's disease: MRI studies. Encyclopedia of neuroscience. Academic Press, In, pp 269–273

Waser M, Garn H (2013) Removing cardiac interference from the electroencephalogram using a modified Pan-Tompkins algorithm and linear regression. Accepted for publication at 35th annual international IEEE EMBS conference.